Available online at www.sciencedirect.com
ScienceDirect
Journal of Power Sources 174 (2007) 648–652
JOURNAL OF POWER SOURCES
www.elsevier.com/locate/jpowsour

Short communication

Electrode materials for ionic liquid-based supercapacitors

Catia Arbizzani, Sabina Beninati, Mariachiara Lazzari, Francesca Soavi, Marina Mastragostino *

Dipartimento di Scienza dei Metalli, Elettrochimica e Tecniche Chimiche, Via San Donato 15, 40127 Bologna, Italy

Available online 29 June 2007

Abstract

The use of ionic liquid (IL) electrolytes is a promising strategy to enhance the performance of supercapacitors above room temperature. In this paper we present the results of a study on optimization of electrode materials for IL-based supercapacitors featuring a hybrid configuration with carbon negative electrode and poly(3-methylthiophene) (pMeT) as positive operating at 60 °C with the ILs *N*-butyl-*N*-methylpyrrolidinium bis(trifluoromethanesulfonyl)imide ($PYR_{14}TFSI$) and 1-ethyl-3-methyl-imidazolium bis(trifluoromethanesulfonyl)imide (EMITFSI). As it concerns the carbon electrode two routes have been pursued: (i) surface modification of commercial activated carbon and (ii) synthesis of mesoporous cryo- and xerogel carbons. Pore size distribution and electrochemical characterization data are related and suggest that the second route should be the most promising for carbons of high specific capacitance and low time constant in IL. For the polymer electrode the nature of the galvanostatic polymerization bath plays a crucial role to provide pMeT of high specific capacitance and the best results may be obtained when pMeT is electropolymerized in the same IL used for the capacitance tests. The strategy of using the acid additive trifluoromethanesulfonimide in IL-based polymerization baths is also described in some detail. This strategy that provides pMeT featuring more than 200 $F\,g^{-1}$ in IL is a clean procedure which prevents consumption of the ionic liquid with great advantage in terms of costs.

Keywords: Hybrid supercapacitor; Ionic liquid; Activated carbon; Xerogel carbon; Cryogel carbon; Poly(3-methylthiophene)

1. Introduction

Supercapacitors for their high specific power are playing a crucial role in transportation, where they can be coupled with lithium batteries or fuel cells to provide power peaks during acceleration as well as for energy recovery during braking of electric vehicles [1–3]. For this application the typical operating temperature is higher than room temperature (RT). Thus, we pursued the strategy of using ionic liquids (ILs) for their high thermal stability, wide electrochemical stability window and good conductivity at RT as "solvent-free" electrolytes in supercapacitors for electric vehicle applications [4–8]. We already demonstrated the viability of this strategy in hybrid supercapacitors with activated carbon (AC) as the negative electrode and poly(3-methylthiophene) (pMeT) as the positive. When a high purity and hydrophobic IL such as *N*-butyl-*N*-methylpyrrolidinium bis(trifluoromethanesulfonyl)imide ($PYR_{14}TFSI$) was used, at 60 °C the AC/IL/pMeT supercapacitor provided maximum cell voltages higher than 3.4 V and specific energy and power of 18 $Wh\,kg^{-1}$ and 14 $kW\,kg^{-1}$, respectively, as well as long cycling stability over 15,000 cycles [6,8]. These results were achieved with commercial negative and positive electrode materials selected for operation in propylene carbonate (PC)-Et_4NBF_4 and that in the IL $PYR_{14}TFSI$ at 60 °C displayed ca. 50% of the specific capacitance exhibited in the conventional organic electrolyte at RT [9]. We demonstrated that improvements of the AC/IL/pMeT performance are feasible if electrodes materials are properly designed in view of their use in the IL [7,8]. Indeed, an IL-based hybrid supercapacitor with electrode materials of specific capacitance increased up to the values exhibited in PC-Et_4NBF_4 and with an IL electrolyte able to provide maximum cell voltage higher than 3.5 V should deliver specific energy higher than 30 $Wh\,kg^{-1}$ [8].

As it concerns the negative electrode, for a high specific capacitance the carbon has to display a high permeability towards the IL to provide a high surface area for the double-layer charging process and this can be obtained by optimization of carbon pore size and surface chemistry. The size of the pores at least should match that of the counterion involved in the double-

* Corresponding author. Tel.: +39 051 2099798; fax: +39 051 2099365.
E-mail address: marina.mastragostino@unibo.it (M. Mastragostino).

0378-7753/$ – see front matter © 2007 Elsevier B.V. All rights reserved.
doi:10.1016/j.jpowsour.2007.06.162

layer formation, thus it should be wider than 1 nm. Furthermore, hydrophilic moieties on the carbon surface are expected to prevent its permeation by ILs with the hydrophobic character required to provide high cycling stability. Mesoporous cryo- and xerogel carbons are particularly promising as IL-based supercapacitor electrodes for their fundamental properties, such as high and tunable mesoporosity, narrow pore-size distribution, high electrical conductivity, hydrophobic surface, which can be controlled by chemical synthesis conditions [10–13]. With respect to aerogel carbons, cryo- and xerogel carbons are more interesting for practical applications in that the supercritical drying step required for the synthesis of aerogel carbons is substituted by freeze or RT drying with great advantage in terms of cost and safety.

As it concerns the conducting polymer, we have already demonstrated that different polymerization conditions affect the pseudocapacitive behaviour of pMeT in the IL, and particularly the electropolymerization in the same IL used for the capacitance tests provides high performance pMeT electrodes [8,14].

In the present paper we report and discuss the results on the development of materials with morphologies and surface chemistry tailored for operation at 60 °C in the hydrophobic ILs $PYR_{14}TFSI$ and 1-ethyl-3-methyl-imidazolium bis (trifluoromethanesulfonyl)imide (EMITFSI). Data on thermal treated activated carbons and cryo- and xerogel carbons of different mesoporosity and on pMeT electropolymerized in ILs by a galvanostatic technique involving the additive trifluoromethanesulfonimide (HTFSI), which provides a clean electrosynthesis procedure, are reported and discussed.

2. Experimental

The cryogel and xerogel carbons were prepared by polycondensation of resorcinol (R, Riedel de Haen, 99.0–100.5%) and formaldehyde (F, 37% aqueous solution, Aldrich) in MilliQ ultrapure water (W, Milli-Q simplicity system, Millipore Co.) with Na_2CO_3 (C, Riedel de Haen, >99.8%) as gelation catalyst, followed by water/*t*-butanol (Fluka, >99.7%) or water/acetone solvent exchange, freeze or RT drying, respectively, and pyrolysis. The R/F molar ratio was 0.5 and the R/C molar ratio and dilution factor D = W/(R + F + C) were 500 and 5.7 for the CRFB5b cryogel carbon and the CRFC5 xerogel carbon and 800 and 2.5 for the CRFB4 cryogel carbon. The initial pH value was 6.4–6.6 and gelation was performed at 85 °C in sealed vessels for at least 3 days. The pyrolysis step, carried out in a furnace (ZE Muffle Furnace) at 1050 °C (2 h, heating rate 10 K min^{-1}, under moderate flux of Argon, 200 cm^3 min^{-1}), was followed by ball milling.

Nitrogen adsorption porosimetry measurements were carried out at 77 K with an ASAP 2020 system (Micromeritics); the carbon powders were dried for at least 2 h at 120 °C before testing. The total specific surface area (S_{BET}) and pore size distribution in the mesopore region of the carbon powders were evaluated from the analysis of the N_2 adsorption isotherms using the B.E.T. and B.J.H. theories.

The carbon electrodes were prepared with 95% (w/w) carbon (PICACTIF activated carbon or cryo/xerogel carbon, ca. 10–15 mg cm^{-2}) and 5% (w/w) polytetrafluoroethylene binder (Du-Pont); the current collectors were carbon coated aluminum grids (Lamart Corp.). Electrodes with pMeT electropolymerized on Pt or glassy carbon (GC) were prepared galvanostatically in a separate-compartment cell (except in the case of polymerization baths based on IL) with Pt counter electrode in ACN (distilled, Fluka)–0.5 M Et_4NBF_4 (Fluka, dried at 80 °C under dynamic vacuum over night)–0.1 M MeT (Aldrich) or in IL–0.1 M HTFSI–0.2 M MeT. Saturated calomel electrode (SCE) or Ag quasi-reference electrode was used to check the electrode potential. The pMeT electrodes with ca. 4 mg cm^{-2} of polymer were electropolymerized at RT with current density i_e = 10–11 mA cm^{-2} and were galvanostatically undoped with current density $i_u = -0.25 i_e$ in order to evaluate the electrochemical stoichiometry of the electropolymerization and, thus, the amount of pMeT polymerized. The HTFSI (Aldrich) was used as received and MeT (Aldrich) was distilled before use. The $PYR_{14}TFSI$ and EMITFSI ILs were dried over night at 100 °C under dynamic vacuum (Büchi Glass Oven B-580) and displayed ca. 30 ppm of water checked by Karl Fisher titration (684 KF Coulometer Metrohm).

Electrochemical characterization of carbon and pMeT-based electrodes was carried out in dry box (MBraun Labmaster 130, H_2O and O_2 < 1 ppm), using Ag quasi-reference electrode and double-layer carbon counter-electrodes with charge storage capability at least double that of the working electrodes; the cells were kept at the controlled temperature of 60 ± 2 °C by a Thermoblock (FALC). The electrochemical tests were performed with a Perkin-Elmer VMP multichannel potentiostat/galvanostat and a Solartron SI 1255 frequency-response analyzer coupled to a 273A PAR potentiostat/galvanostat. The specific capacitance was evaluated by cyclic voltammetry (CV) at 20 mV s^{-1} and the data were estimated from the slope of the integral over time of the discharge voltammetric current versus electrode potential plot; the maximum electrode potential sweep was −1.9/0.3 V versus Ag and 1.4/−0.5 V versus Ag for the carbon and the polymer electrode, respectively. Impedance spectra were recorded with 5 mV AC perturbation in the frequency range 10 kHz to 10 mHz taking 10 points per decade.

Scanning electron microscopy (SEM) observations were carried out with a ZEISS EVO 50 instrument.

3. Results and discussion

3.1. Carbon negative electrodes

Table 1 and Fig. 1 report some results of the porosity analysis and of the electrochemical characterization of the carbons which we investigated. Table 1 shows the specific surface area (S_{BET}) and the mean pore diameter in the mesopore region (d_{meso}), as well as the specific capacitance in the ILs $PYR_{14}TFSI$ and EMITFSI at 60 °C from CVs of the commercial activated carbon (AC), of the AC carbon treated under Ar atmosphere (200 cm^3 min^{-1}) at 1050 °C for 2 h (ACT) and of the cryo/xerogel carbons CRFB4, CRFC5 and CRFB5b. Fig. 1 shows the specific cumulative surface area in the mesopore region as evaluated from the widest to the smallest pores versus

Table 1
Specific surface area (S_{BET}), mean pore diameter in the mesopore region (d_{meso}) of the carbon powders and specific capacitance from CV at 20 mV s^{-1} in the ILs $PYR_{14}TFSI$ and EMITFSI at 60 °C of the carbon electrodes

Carbon	S_{BET} ($m^2\,g^{-1}$)	d_{meso} (nm)	Specific capacitance ($F\,g^{-1}$)	
			$PYR_{14}TFSI$	EMITFSI
AC	2480	3	50	85
ACT	1960	3	87	107
CRFB4	465	9	–	52
CRFC5	550	15	–	56
CRFB5b	610	20	–	61

pore diameter. The activated carbon AC displays a very high S_{BET} and, as evidenced in Fig. 1, a high mesopore specific surface which corresponds to ca. 45% of S_{BET} and originates from pores with mean diameter of ca. 3 nm. Despite this suitable morphology, with pores large enough to be filled with the ILs, the carbon displays a specific capacitance lower, particularly in $PYR_{14}TFSI$, than the value expected on the basis of the typical capacitance of a clean graphite surface, i.e. 20–30 μF cm^{-2}, thus suggesting that a low percentage of the AC's mesopore area is accessible by the ILs. This could be explained with the presence of surface moieties which often occur in activated carbons as oxygen functional groups (carboxyl, hydroxyl,...) and which repel the two hydrophobic ILs. It has been demonstrated that such functionalities decompose almost quantitatively at 1000 °C under inert gas [15], thus we treated the AC carbon at 1050 °C in Ar atmosphere and we obtained the ACT carbon with a slightly lower surface area and the same percentage of mesopore distribution, but a significantly higher specific capacitance than the AC carbon in both the ILs and such increase was higher in $PYR_{14}TFSI$ than in EMITFSI, as evidenced in Table 1. Thus, such treatment modifies the carbon surface chemistry and increases the compatibility of the ACT carbon with the ILs, providing up to 107 F g^{-1} in EMITFSI. The fact that the AC and ACT carbons display higher specific capacitance in EMITFSI than in $PYR_{14}TFSI$ may be related to the different chemistry of the EMI^+ and $PYR_{14}{}^+$ cations which display not only different steric hindrance but also different polarizability as suggested by the different conductivity at 60 °C of the corresponding EMITFSI and $PYR_{14}TFSI$ ILs of 25 and 6 mS cm^{-1}, respectively [6,7,16]. However, it should be mentioned that the $PYR_{14}TFSI$ features a wider electrochemical stability window than that of EMITFSI [7,17], and this could be an advantage for application in high-voltage supercapacitors.

Given that also in the ACT carbon the main part of the S_{BET} surface is not used for the double-layer charging process, we pursued the strategy of investigating the mesoporous cryo- and xerogel carbons CRFB4, CRFC5, and CRFB5b. In Table 1 their S_{BET} values range from 465 to 610 $m^2\,g^{-1}$ with the 40–50% originating from mesopores centered at 9, 15 and 20 nm and their specific capacitance at 60 °C in EMITFSI is in the range of 50–60 F g^{-1}, corresponding to 20–30 μF cm^{-2} of mesoporous surface area, thus indicating that in these carbons all the mesopore surface is used for the double-layer charging process, and that carbon surface is easily accessed by the IL.

This corresponds also to a low electrode charging resistance which is a very important feature for supercapacitor application as evidenced in Fig. 2 which shows the Nyquist plots recorded in EMITFSI at −1.0 V versus Ag for ACT and CRFB5b electrodes with almost the same amount of carbon. The high frequency

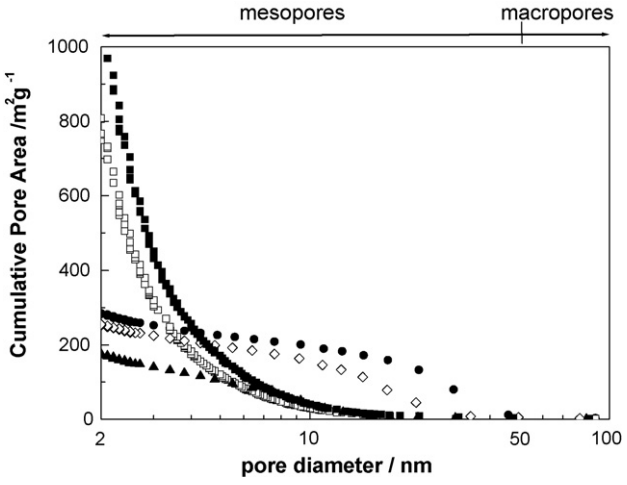

Fig. 1. Specific cumulative pore area vs. mesopore diameter of the (■) AC, (□) ACT, (▲) CRFB4, (◊) CRFC5, and (●) CRFB5b carbons.

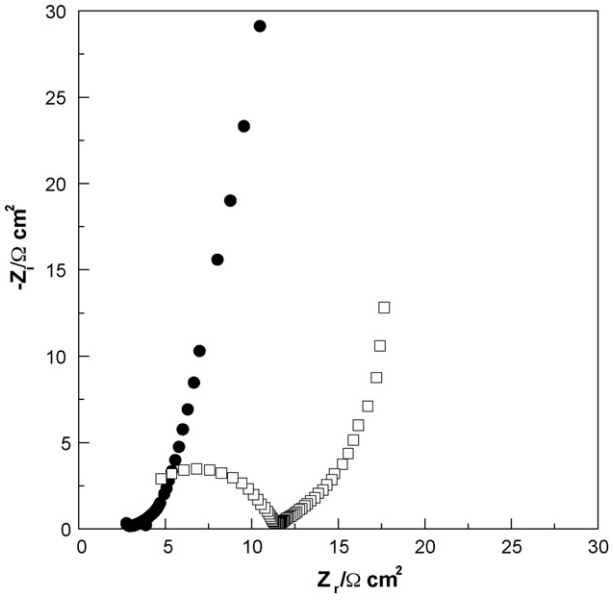

Fig. 2. Nyquist plots recorded in EMITFSI at −1.0 V vs. Ag of (□) ACT and (●) CRFB5b carbon electrodes.

Table 2
Specific capacitance from CV at 20 mV s^{-1} in the ILs $PYR_{14}TFSI$ and EMITFSI at 60 °C of pMeT galvanostatically electropolymerized at RT in different electropolymerization baths (3.3–4.5 mg cm^{-2} of pMeT)

Polymerization bath	Specific capacitance (F g^{-1})	
	$PYR_{14}TFSI$	EMITFSI
ACN-Et_4NBF_4-MeT	135	–
ACN-LiTFSI-MeT	100	135
$PYR_{14}TFSI$-HTFSI-MeT	225	–
EMITFSI-HTFSI-MeT	–	250

semicircle in the spectrum of the ACT carbon, related to electronic and ionic resistances between the smallest mesopores in parallel with the double-layer capacitance of the carbon outer surface, is absent in the CRFB5b's. Thus, work is in progress in our laboratory to synthesize by proper selection of the gelation bath composition cryo/xerogel carbons with mesoporous surface $\geq 500\,F\,g^{-1}$, which should outperform activated carbons providing $100\,F\,g^{-1}$ at a lower time constant.

3.2. Polymer positive electrodes

Table 2 reports the specific capacitance values in the two ILs at 60 °C of pMeT galvanostatically polymerized in different electropolymerization baths. Table 2 evidences that the substitution of ACN-based polymerization bath with those based on the same ILs used for the following capacitance tests provides specific capacitance values higher than $200\,F\,g^{-1}$. Particularly, the values of 225 and $250\,F\,g^{-1}$ are obtained with $PYR_{14}TFSI$ and EMITFSI electrolytes, respectively. This can be related to the different morphology exhibited by pMeT when the ACN-based bath is substituted by that with the IL, as evidenced in Fig. 3, which reports the SEM images of pMeT electropolymerized in ACN-LiTFSI and in $PYR_{14}TFSI$. Table 2 evidences that also in the case of the polymer electrodes the highest specific capacitance values are obtained with the EMITFSI IL.

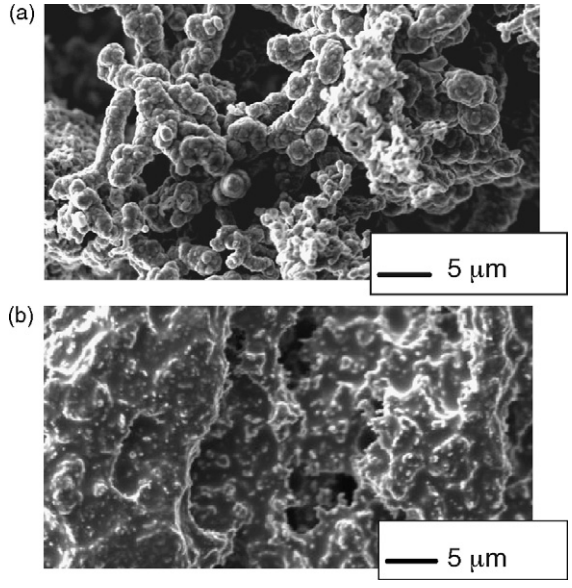

Fig. 3. SEM images of pMeT electropolymerized in (a) ACN-LiTFSI-MeT and in (b) $PYR_{14}TFSI$-HTFSI-MeT.

The main drawback with galvanostatic preparation of large quantities of polymer in ILs is the formation of byproducts at the counter electrode which typically poison the polymerization bath. Thus, to control the cathodic reaction we pursued the strategy to add the acid HTFSI which dissociates to give the same anion $TFSI^-$ of the IL and the proton which in turn gives H_2 at the counter electrode while anodic polymerization takes place at the working. This clean procedure which does not modify the chemistry of the electrosynthesis solution is described by the following overall electrochemical reaction in which a stoichiometry of $2.3\,F\,mol^{-1}$ of polymerized MeT monomer unit ($CH_3C_4H_3S$) is considered:

$$0.3n\mathrm{HTFSI} + n\mathrm{CH_3C_4H_3S} \rightarrow (CH_3C_4HS^{0.3+}\mathrm{TFSI}_{0.3}{}^-)_n + 1.15n\mathrm{H_2} \quad (1)$$

From this stoichiometry 0.3 mol of HTFSI per mol of polymerized monomer unit provide that the IL is not consumed because they supply the required amount of the p-doping anion $TFSI^-$ and the protons which are reduced to H_2 along with those delivered by the polymerization reaction (2 mol of H^+ per mol of polymerized monomer unit) [14].

Fig. 4 reports the voltage profiles of the working and counter electrodes upon the galvanostatic electropolymerization of pMeT and the undoping process in $PYR_{14}TFSI$-HTFSI-MeT at RT (stirred solution) from which an electrochemical stoichiometry of $2.28\,F\,mol^{-1}$ of polymerized monomer unit has been evaluated. During polymerization the potentials of the working and counter electrode are quite stable at ca. 1.5 and −0.3 V versus Ag, respectively, which correspond to the monomer oxidation and the H^+ reduction as evidenced by Fig. 5 which displays the first linear sweep voltammetries at 20 mV s^{-1} and RT of a Pt electrode in $PYR_{14}TFSI$, $PYR_{14}TFSI$-HTFSI and $PYR_{14}TFSI$-HTFSI-MeT. Therefore, the pMeT polymerization at the working electrode is balanced by the reduction of the acid proton of HTFSI at the counter electrode. This novel galvanostatic polymerization procedure, which can be extended to prepare other polymers in ILs, does not waste the IL offering great advantage in terms of costs.

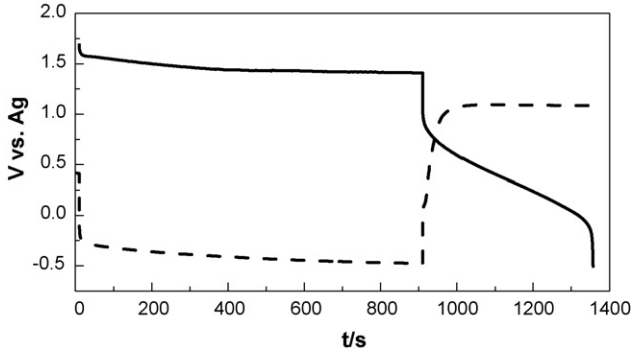

Fig. 4. Voltage profiles of the working electrode (GC, solid line) and the counter electrode (Pt, dashed line) upon the galvanostatic electropolymerization of pMeT at 11.3 mA cm^{-2} and the undoping process at −2.8 mA cm^{-2} in $PYR_{14}TFSI$-HTFSI-MeT at RT.

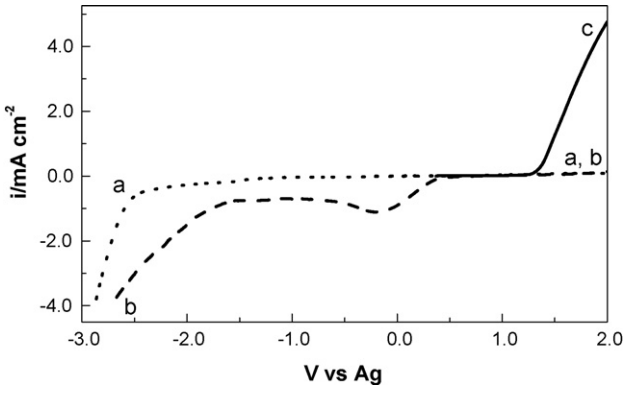

Fig. 5. Linear sweep voltammetries at 20 mV s^{-1} and RT of a Pt electrode in (a) $PYR_{14}TFSI$, in (b) $PYR_{14}TFSI$-HTFSI and (c) $PYR_{14}TFSI$-HTFSI-MeT.

4. Conclusions

With this study we have identified some routes to optimize electrode materials for hybrid supercapacitor with hydrophobic IL electrolytes and, following such routes, we have developed carbon and polymer electrode materials featuring at 60 °C up to 107 and 250 F g^{-1} in EMITFSI and 87 and 225 F g^{-1} in $PYR_{14}TFSI$, respectively. Thermal treatment at 1050 °C in Ar atmosphere of activated carbons removes/modifies the surface moieties generally present in such carbons and allows a better permeability by each IL, thus increasing the accessible surface for the double-layer charging process. A more promising strategy should be the development of cryo/xerogel carbons of mesopore specific surface area > 500 m^2 g^{-1}, which should display at least 100 F g^{-1} on the basis of the values of 20–30 μF cm^{-2} of mesoporous surface featured by the CRFB4, CRFC5, and CRFB5b carbons, with a low electrode charging resistance. As it concerns the polymer electrode, the novel galvanostatic polymerization in IL involving the acid additive HTFSI is a clean procedure which yields pMeT featuring 225 and 250 F g^{-1} in $PYR_{14}TFSI$ and EMITFSI ILs, with advantage in terms of costs because the IL is not wasted by counter electrode reaction nor consumed to balance the pMeT p-doping charge.

Acknowledgements

Research funded by ILHYPOS UE Project (TST4-CT-2005-518307, Contract Number 518307). ENEA-IDROCOMB (Casaccia, Italy) and Degussa-Creavis Technologies & Innovation (Marl, Germany) are acknowledged for providing the $PYR_{14}TFSI$ and EMITFSI ILs, respectively.

References

[1] A. Chu, P. Braatz, J. Power Sources 112 (2002) 236.
[2] P. Rodatz, G. Paganelli, A. Sciarretta, L. Guzzella, Con. Eng. Prac. 13 (2005) 41.
[3] R.J. Brodd, K.R. Bullock, R.A. Leising, R.L. Middaugh, J.R. Miller, E. Takeuchi, J. Electrochem. Soc. 151 (2004) K1.
[4] D. Adam, Nature 407 (2000) 938.
[5] A. Balducci, U. Bardi, S. Caporali, M. Mastragostino, F. Soavi, Electrochem. Commun. 6 (2004) 566.
[6] A. Balducci, W.A. Henderson, M. Mastragostino, S. Passerini, P. Simon, F. Soavi, Electrochim. Acta 50 (2005) 2233–2237.
[7] A. Balducci, F. Soavi, M. Mastragostino, Appl. Phys. A 82 (2006) 627–632.
[8] C. Arbizzani, A. Balducci, M. Mastragostino, S. Passerini, P. Simon, F. Soavi, ECS Trans. 1 (2006) 55–59.
[9] A. Laforgue, P. Simon, J.F. Fauvarque, M. Mastragostino, F. Soavi, J.F. Sarrau, P. Lailler, M. Conte, E. Rossi, S. Saguatti, J. Electrochem. Soc. 150 (2003) A645–A651.
[10] S.A. Al-Muhtaseb, J. Ritter, Adv. Mater. 15 (2003) 101–114.
[12] E. Frackowiak, F. Beguin, Carbon 39 (2001) 937–950.
[13] A.G. Pandolfo, A.F. Hollenkamp, J. Power Sources 157 (2006) 11–27.
[14] C. Arbizzani, F. Soavi, M. Mastragostino, J. Power Sources 162 (2006) 735–737.
[15] H.P. Boehm, Carbon 32 (1994) 759–769.
[16] A.B. McEwen, H.L. Ngo, K. LeCompte, J.L. Goldman, J. Electrochem. Soc. 146 (1999) 1687–1695.
[17] H. Sakaebe, H. Matsumoto, Electrochem. Commun. 5 (2003) 594–598.